



1 **Two-wavelength thermo-optical determination of Light Absorbing Carbon in**
2 **atmospheric aerosols**

3
4 Dario Massabò^{1,*}, Alessandro Altomari², Virginia Vernocchi¹, Paolo Prati¹

5
6 1: Dept. of Physics, University of Genoa & INFN, Via Dodecaneso 33, 16146, Genova, Italy

7 2: Dept. of Physics, University of Genoa, Via Dodecaneso 33, 16146, Genova, Italy

8
9 **Abstract**

10
11 Thermo-optical analysis is widely adopted for the quantitative determination of Total, TC,
12 Organic, OC, and Elemental, EC, Carbon in atmospheric aerosol sampled by suitable filters.
13 Nevertheless, the methodology suffers of several uncertainties and artefacts as the well-known
14 issue of charring affecting the OC-EC separation. In the standard approach, the effect of the
15 possible presence of Brown Carbon, BrC, in the sample is neglected. BrC is a fraction of OC,
16 usually produced by biomass burning with a thermic behaviour intermediate between OC and
17 EC. BrC is optically active: it shows an increasing absorbance when the wavelength moves to
18 the blue/UV region of the electromagnetic spectrum. Definitively, the thermo-optical
19 characterization of carbonaceous aerosol should be reconsidered to address the possible BrC
20 content in the sample under analysis.

21 We introduce here a modified Sunset Lab Inc. EC/OC Analyzer. Starting from a standard
22 commercial set-up, the unit has been modified at the Physics Department of the University of
23 Genoa (IT), making possible the alternative use of the standard laser diode at $\lambda = 635$ nm and
24 of a new laser diode at $\lambda = 405$ nm. In this way, the optical transmittance through the sample
25 can be monitored at both the wavelengths. Since at shorter wavelengths the BrC absorbance is
26 higher, a better sensitivity to this species is gained. The modified set-up also gives the
27 possibility to quantify the BrC concentration in the sample at both the wavelengths. The new
28 unit has been thoroughly tested, with both artificial and real-world samples: the first
29 experiment, in conjunction with the Multi Wavelength Absorbance Analyzer (MWAA,
30 Massabò et al., 2013 and 2015), resulted in the first direct determination of the BrC Mass
31 Absorption Coefficient (MAC) at $\lambda = 405$ nm: $MAC = 23 \pm 1 \text{ m}^2 \text{ g}^{-1}$.

32
33 **Keywords:** carbonaceous aerosol, brown carbon, thermo-optical analysis, mass absorption
34 coefficient
35
36

* Corresponding Author: massabo@ge.infn.it



37 **1. Introduction**

38

39 Light absorbing carbon (LAC) is the fraction of carbonaceous aerosol, which can absorb
40 electromagnetic radiation in the visible or near-visible range (Pöschl, 2003; Bond and
41 Bergstrom, 2006; Moosmüller et al., 2009; Ferrero et al., 2018). A wide literature investigates
42 and characterizes the optical properties of the inorganic-refractory LAC fraction, usually
43 referred as Black Carbon, BC, (e.g. Bond et al., 2013; and reference therein) which is strongly
44 absorbing from UV to IR, with a weak dependence on wavelength (Bond and Bergstrom, 2006;
45 Moosmüller et al., 2009). Much less studied and understood is the organic LAC, often labelled
46 as Brown Carbon, which appears to be optically active at wavelengths shorter than 650 nm and
47 with an increasing absorbance moving to the blue and ultraviolet (UV) range (Pöschl, 2003;
48 Andreae and Gelencsér, 2006; Moosmüller et al., 2011; Laskin et al., 2015; Olson et al., 2015).
49 BrC can therefore be considered as the “optically active” part of the OC dispersed in the
50 atmosphere. When considered from a thermo-chemical point of view, BrC also shows a
51 refractory behaviour since, in an inert atmosphere, it volatilizes at temperatures greater than 400
52 °C only (Chow et al., 2015). A discussion on the sources of atmospheric LAC is outside the
53 scope of the present work; we simply remind that it is produced mainly by biomass burning,
54 even if in some cases also incomplete combustion of fossil fuels used in transport activities
55 (i.e. terrestrial vehicles, ships and aircrafts) can generate this kind of compounds (Corbin et al,
56 2018). It is also worth to underline that carbonaceous aerosols impact on human health (Pope
57 and Dockery, 2006; Chow et al., 2006; Mauderly and Chow, 2008), as well as on climate and
58 environment (Bond and Sun, 2005; Highwood and Kinnersley, 2006; Chow et al., 2010).

59 In the wider landscape of atmospheric carbonaceous aerosol, despite a worldwide diffused
60 effort, the situation is not satisfactory and a standardized and conclusive approach is still
61 missing. The quantitative determination of TC, OC and EC is often performed by a thermo-
62 optical analysis (Birch and Cary, 1996; Watson et al., 2005; Hitzenberger et al., 2006) of
63 aerosol samples collected on quartz fibre filters. However, thermo-optical analyses are affected
64 by several issues and artefacts (Yang and Yu, 2002; Chow et al., 2004) and different
65 laboratories/agencies adopt protocols which systematically result in discrepancies, particularly
66 large in the EC quantification (Birch and Cary, 1996; Chow et al., 2007; Cavalli et al., 2010).
67 A further issue arises when the effects of the possible presence of BrC in the sample are taken
68 into account. So far, the monitoring of the sample transmittance during the thermal cycle, has
69 been introduced to correct for the well know charring effect and the formation of pyrolytic
70 carbon (Birch and Cary, 1996). This implies that BC is the sole absorbing compound at the



71 wavelength implemented in the thermo-optical analyser (for instance at $\lambda = 635$ nm, the
72 wavelength of the laser diode mounted in the extremely diffused Sunset Lab. Inc. EC/OC
73 analyzer). Basically, with a sizeable concentration of BrC in the sample, one of the key
74 assumptions of the thermo-optical methods fails and the EC/OC separation is even more
75 unstable (to not say that, by design, the BrC quantification is not possible). This issue was
76 preliminarily addressed by (Chen et al., 2015) by a multi-wavelength TOT/TOR instrument
77 (Thermal Spectral Analysis – TSA) and further investigated in (Massabò et al., 2016). In the
78 latter work, a method to correct the results of a standard Sunset analyzer and to retrieve the
79 BrC concentration in the sample was introduced. The achievement was possible thanks to a
80 synergy with the information provided by the Multi Wavelength Absorbance Analyzer,
81 MWAA, (Massabò et al., 2015) developed in the same laboratory. A further step towards BrC
82 quantification through the utilization of TSA was discussed in (Chow et al., 2018), where it
83 was proved that the use of 7-wavelengths in thermal/optical carbon analysis allows
84 contributions from biomass burning and secondary organic aerosols to be estimated. It is
85 worthy to note that the biomass burning contribution to PM concentration can be also estimated
86 by other methods such as Aerosol Mass Spectrometry, AMS (Daellenbach et al., 2016).

87 The MWAA approach allows the determination of the spectral dependence of the aerosol
88 absorption coefficient (b_{abs}) which can be generally described by the power-law relationship
89 $b_{\text{abs}}(\lambda) \sim \lambda^{-\text{AAE}}$, where the AAE is the Ångström Absorption Exponent. Several works reported
90 AAE values which depend on the aerosol chemical composition (Kirchstetter et al., 2004; Utry
91 et al., 2013) as well as its size and morphology (Lewis et al., 2008; Lack et al., 2012; Lack and
92 Langridge, 2013; Filep et al., 2013; Utry et al., 2014). Furthermore, the spectral dependence of
93 the aerosol has been exploited to identify different sources of carbonaceous aerosol (e.g.
94 Sandradewi et al., 2008; Favez et al., 2010; Lack and Langridge, 2013; Massabò et al., 2013
95 and 2015). In general, AAE values close to 1.0 have been found to be related to urban PM
96 where fossil fuels combustion is dominant, while higher AAE values, up to 2.5, have been
97 linked to carbonaceous aerosols produced by wood burning (Harrison et al., 2013; and
98 references therein) and therefore to the presence of BrC.

99 In the previous work by (Massabò et al., 2016) the effect of the BrC possibly contained in
100 the sample on the thermo-optical analysis was quantified and exploited to retrieve the BrC
101 concentration from the raw data provided by a standard Sunset Lab. Analyzer. This first step,
102 suggested to modify/upgrade a Sunset unit adding the possibility to use a second laser diode in
103 the blue range. This improves the sensitivity to the BrC and allows to check whether the BrC



104 quantification depends on the adopted wavelength. We finally followed this route and we here
105 introduce our modified Sunset Analyzer unit, the validation tests and the results of the first
106 campaign in which the new unit was deployed.

107

108 **2. Materials and Methods**

109

110 **2.1 The 2-lambda SUNSET analyzer**

111 We have modified a commercial Thermal Optical Transmittance (TOT) instrument (Sunset
112 Lab Inc.). This equipment had been originally designed (Birch and Cary, 1996) with a red laser
113 diode ($\lambda = 635$ nm) to have the possibility to monitor and correct the well know problem of
114 the formation of pyrolytic carbon by charring (Birch and Cary, 1996; Bond and Bergstrom,
115 2006; Chow et al., 2007; Cavalli et al., 2010). The hypothesis under such choice was that the
116 OC is optically inactive at wavelengths greater than 600 nm and therefore the laser beam
117 attenuation is only due to the EC originally present or formed by charring in the sample under
118 analysis. Actually, even at this wavelength, BrC can affect the reliability of the OC/EC
119 separation and the standard methodology can be modified to quantify the BrC concentration
120 (Massabò et al., 2016). Nevertheless, at $\lambda = 635$ nm the BrC Mass Absorption Coefficient,
121 MAC(BrC), remains much smaller of the corresponding MAC(BC) and the modified
122 procedure could/should be implemented at shorter wavelengths to gain in sensitivity.

123 We have modified our SUNSET unit making possible the alternative use of the standard
124 laser diode at $\lambda = 635$ nm or of a World Star Technologies, 100 mW, laser diode at $\lambda = 405$
125 nm. This second laser diode can be mounted on the top of the SUNSET furnace by a homemade
126 adapter (see Figure 1) and easily exchanged with the native red diode. With the new laser
127 diode, the light detector placed at the bottom of the SUNSET furnace has to be changed too
128 and we selected a photodiode (PD) THORLABS FDS1010 coupled with a bandpass filter
129 THORLABS FBH405-10. The responsivity of the PD FDS1010 around $\lambda = 400$ nm is quite
130 low (about 50 mA W^{-1}) but the high power delivered by the laser diode results in signals with
131 an amplitude comparable to the values measured with the original SUNSET set-up.
132 Furthermore, the FBH405-10 filter cuts all the light background produced by the high
133 temperature of the SUNSET furnace, thus preserving the signal-to-noise ratio. Both laser and
134 PD can be exchanged in about 10 min and no particular attention is requested but the proper
135 alignment to maximize the PD output signal (i.e. the *transmittance* value displayed by the
136 SUNSET control software). We have to note that the original configuration of the SUNSET



137 instrument adopts a lock-in amplifier to improve the signal-to-noise ratio of the PD: we did not
138 have the possibility to manipulate the parameters of the lock-in amplifier and to tune it to the
139 new configuration.

140

141 **2.2 Test of the new configuration**

142 The new set-up of the Sunset Analyzer was tested using both synthetic and real samples,
143 collected on quartz fibre filters. Synthetic samples were prepared starting with a 5% (volume)
144 solution of Aquadag, then nebulised by a Blaustein Atomizer (BLAM) and collected on quartz
145 fibre filters. Aquadag is the trade name of a water-based colloidal graphite coating (particle
146 diameters between 50 and 100 nm): these samples can therefore be considered to be composed
147 by EC/BC only. The samples were first sent to an optical characterization by the MWAA
148 instrument (Multi Wavelength Absorbance Analyzer, Massabò et al., 2015) which
149 demonstrated that the optical absorption of Aquadag is independent on the wavelength.
150 Actually, Aquadag particles tend to form conglomerates on the filters surface, with dimension
151 about double of the longer wavelength implemented in the MWAA (i.e. the 850 nm of the
152 infrared laser diode; Massabò et al., 2015). So, the comparison between the two Sunset set-ups
153 was made with samples having the same absorption properties. EC and TC quantifications
154 obtained at $\lambda = 635$ nm and $\lambda = 405$ nm resulted compatible adopting both the NIOSH5040 and
155 EUSAAR_2 protocol (Cavalli et al., 2010), as shown in Figure 2 for the whole set of synthetic
156 samples.

157 A second set of synthetic samples was prepared to mimic the behaviour of real-world aerosol
158 samples: a 3% (weight) solution of ammonium sulphate $(\text{NH}_4)_2\text{SO}_4$ in Aquadag was prepared
159 and nebulized with the BLAM. This way, a scattering compound is mixed to the absorbing
160 Aquadag spherules. The optical absorption measured with MWAA resulted independent on
161 wavelength with this second set of samples too. The results of the Sunset analysis with both
162 the red and blue laser set-up are shown in Figure 3. This second set of samples was analysed
163 through the EUSAAR_2 protocol only. A strong correlation between the TC and EC values
164 measured in red and blue light was obtained again with a slope close to unit.

165 A third and final test was performed using a set of daily PM₁₀ samples collected by a low-
166 volume sampler (TCR - Tecora, Italy) on quartz fibre filters (Pall-2500 QAO-UP, 47 mm
167 diameter) in spring 2016 in the urban area of the city of Genoa (IT). A previous and long set
168 of similar campaigns addressed to PM₁₀ characterization (e.g. Bove et al., 2014 and references
169 therein) in the same urban area could not identify sizeable contributes of biomass burning to
170 PM composition, in particular during spring and summer. Such situation was confirmed by the



171 determination of the Ångström exponent in the present samples by the MWAA. Actually, in
172 the set of twenty PM₁₀ samples, the values of the Ångström exponent ranged between 0.9 and
173 1.2, this confirming that Black Carbon is the sole or totally dominant light absorbing
174 component in the local PM₁₀ (Sandradewi et al., 2008; Harrison et al., 2013). Half of the
175 samples was then sent to the Sunset analysis by the NIOSH5040 protocol while the
176 EUSAAR_2 protocol was adopted for the remaining subset. The results are shown in Figure 4.
177 The EC concentration values measured with the standard and modified Sunset analyzer are
178 fully compatible when the NIOSH5040 protocol is adopted (basically, the split point position
179 in the Sunset thermogram does not change with the two laser diodes). Instead, EC values
180 determined by the EUSAAR_2 protocol resulted lower by about 30% when the blue laser diode
181 was mounted. This corresponds to a shift of the split point position, which moves right and thus
182 increases the amount of carbonaceous aerosol counted in the OC fraction. This effect is linked
183 to the well-known issue of the formation of pyrolytic carbon during the thermal cycle in the
184 inert atmosphere (i.e. in He). Several literature studies (e.g.: Cavalli et al., 2010; Panteliadis et
185 al., 2015) indicated that the charring is smaller at the higher temperatures reached during the
186 NIOSH thermal protocol. On the other way, standard thermo-optical analyses of urban PM
187 samples often give higher EC values (up to 50%) when performed following the EUSAAR_2
188 instead of higher-temperature protocols (Subramanian et al., 2006; Zhi et al., 2008; Piazzalunga
189 et al., 2011; Karanasiou et al., 2015; Panteliadis et al., 2015). Furthermore, as by-product of
190 previous PM₁₀ studies in the urban area of Genoa by a standard Sunset unit, we could observe
191 a systematic and very reproducible 40% discrepancy between EC values determined in the
192 same samples by EUSAAR_2 and NIOSH5040 protocols (with EC:EUSAAR > EC:NIOSH).
193 Therefore, the thermo-optical analysis in blue light seems to be more sensitive to the charring
194 formation during the EUSAAR_2 protocol and thus possibly more reliable in the EC/OC
195 separation.

196

197 **3. First field campaign and results**

198

199 The modified Sunset set-up was used for the first time, in conjunction with the MWAA
200 instrument and apportionment methodology (Massabò et al., 2015), to retrieve the MAC (Mass
201 Absorption Coefficient) of Brown Carbon at the two wavelengths of $\lambda = 635$ nm and $\lambda = 405$
202 nm, in a set of samples collected wintertime in a mountain site.

203

204 **3.1 Samples collection**



205 Aerosol samples were collected in a small village (Propata, 44°33'52.93''N, 9°11'05.57''E,
206 970 m a.s.l.) situated in the Ligurian Apennines, Italy. Three different sets of PM₁₀ aerosol
207 samples were collected by a low-volume sampler (38.3 l min⁻¹ by TCR Tecora): the first and
208 the third sets had filter change set every 24h while the second set was sampled on a 48h-basis.
209 In total, 41 (14+13+14) PM₁₀ samples were collected on quartz-fibre filters (Pall, 2500QAO-
210 UP, 47 mm diameter), between February 2nd and April 19th, 2018. Before the sampling, the
211 filters were baked at T = 700°C for 2 hours to remove possible internal contamination. Field
212 blank filters were used to monitor possible contaminations during the sampling phase. Wood
213 burning is one of the PM sources around the sampling site, especially during the cold season,
214 as it is used for both domestic heating and cooking purposes.

215

216 **3.2 Laboratory analyses**

217 All the samples were weighed before and after sampling in an air-conditioned room (T = 20
218 ± 1 °C; R.H. = 50 % ± 5%), after 48h conditioning. The gravimetric determination of the PM
219 mass was performed using an analytical microbalance (precision: 1 µg) which was operated
220 inside the conditioned room; electrostatic effects were avoided by the use of a de-ionizing gun.

221 After weighing, samples were first optically analyzed by MWAA to retrieve the absorption
222 coefficient (b_{abs}) of PM at five different wavelengths. The EC and OC determination was
223 performed adopting the EUSAAR_2 protocol (Cavalli et al., 2010) with both laser diodes at λ
224 = 635 nm and at $\lambda = 405$ nm (two different punches were extracted from each filter sample).

225 Finally, the remaining portion of the same quartz-fibre filters underwent a chemical
226 determination of the Levoglucosan (1,6-Anhydro-beta-glucopyranose) concentration by High
227 Performance Anion Exchange Chromatography coupled with Pulsed Amperometric Detection
228 (Piazzalunga et al., 2010). As well known in literature, this sugar is one of the typical marker
229 of biomass burning (Vassura et al., 2014).

230

231 **3.3 Optical apportionment**

232 The MWAA analysis provided the raw data to measure the spectral dependence of the
233 aerosol absorption coefficient (b_{abs}) which can be generally described by the power-law
234 relationship $b_{\text{abs}}(\lambda) \sim \lambda^{-\text{AAE}}$ where AAE is the Ångström Absorption Exponent.

235 The time series of the resulting AAE values is shown in Figure 5: they range between
236 1.05 and 1.96 with a mean value of 1.55 ± 0.21 . This figure indicates a substantial presence of
237 wood burning in the sampling area. In (Massabò et al., 2015 and Bernardoni et al, 2017), an



238 optical apportionment model (the “MWAA model”) based on the measurement of b_{abs} at five
239 wavelengths had been introduced to obtain directly the BrC AAE (α_{BrC}) and the BrC absorption
240 coefficient ($b_{\text{abs}}^{\text{BrC}}$) at each measured wavelength. It is worthy to note that, at the basis of the
241 MWAA model, there is the assumption that BrC is produced by wood combustion only (see
242 §4 in Massabò et al., 2015; Zheng et al., 2013). In Figure 5, we report the optical apportionment
243 at $\lambda = 635$ nm and at $\lambda = 405$ nm i.e. at the wavelength of the two laser diodes used in our
244 modified Sunset instrument. At $\lambda = 635$ nm, light absorption resulted mainly due to BC from
245 both fossil fuel (FF) and biomass burning (WB) and the $b_{\text{abs}}^{\text{BrC}}$ average value is 15% of total
246 b_{abs} , with the notable exception of some days in which it reached values of $\sim 30\%$, in
247 correspondence of $\text{AAE} > 1.9$. Instead, at $\lambda = 405$ nm, the BrC contribute to light absorption
248 rises up to 33% (average percentage of total b_{abs}), with a maximum value of 51%, again when
249 $\text{AAE}_{\text{exp}} > 1.9$. The time series of $b_{\text{abs}}^{\text{BrC}}$ values at both the wavelengths turned out to be well
250 correlated ($R^2 = 0.71$) with the Levoglucosan (*Levo*, in the following) concentration values, as
251 reported in Figure 6. The slope of the correlation curve increases by a factor 5.8 when moving
252 from the red to the blue light.

253 The average α_{BrC} value turned out to be $\alpha_{\text{BrC}} = 3.9 \pm 0.1$, in very good agreement with a
254 previous value ($\alpha_{\text{BrC}} = 3.8 \pm 0.2$) obtained in the same site and with the same approach
255 (Massabò et al., 2016). The result is also in agreement with other literature works (Yang et al.,
256 2009; Massabò et al., 2015; Chen et al., 2015).

257

258 **3.4 Brown Carbon MAC**

259 The methodology to extract the MAC value for BrC by the coupled used of MWAA and
260 Thermo-Optical Analysis has been introduced in a previous work (Massabò et al., 2016). In
261 that case, a standard (i.e.: with a red laser diode only) Sunset unit was used. The entire
262 procedure is described in details in (Massabò et al., 2016), here we briefly summarize the main
263 steps:

- 264 a) The fraction of light attenuation due to the BrC is first calculated in each sample with
265 the MWAA raw data.
- 266 b) The empirical relationship between the light attenuation through the sample, observed
267 in the MWAA and Sunset set-ups is then determined. We remind that in the Sunset set-
268 up, the light attenuation is continuously recorded during the analysis; the value
269 characteristic of each blank filter can be retrieved when all the light absorbing PM has
270 been volatilized (i.e. at the end of the thermal protocol).



- 271 c) The fraction of light attenuation due to the BrC in the sample is therefore calculated for
272 the Sunset set-up and the initial transmittance value is corrected to estimate the
273 attenuation value that it would have been found if BrC were not present in the filter
274 sample.
- 275 d) A new split-point position is then determined taking into account the corrected value of
276 the initial transmittance.
- 277 e) The OC and EC values determined with the standard and corrected split-point positions
278 are then compared and the difference ($OC_{cor} - OC_{std} = EC_{std} - EC_{cor}$) is operatively
279 assumed to be equal to the BrC in the sample. The corresponding BrC atmospheric
280 concentration is finally calculated.
- 281 f) The correlation between the values of b_{abs}^{BrC} , provided by the MWAA analysis (see
282 section 3.3) and BrC concentration, is studied to determine the MAC value.

283

284 In the present experiment, the procedure was adopted to analyse the thermograms produced
285 with both the red and the blue laser diode mounted in the Sunset unit: the results are
286 summarized in Figure 7. Despite a rather high noise in the data, the MAC(BrC) value at the
287 two wavelengths can be determined and it turns out to be $MAC(BrC) = 9.8 \pm 0.4 \text{ m}^2 \text{ g}^{-1}$ and 23
288 $\pm 1 \text{ m}^2 \text{ g}^{-1}$, respectively at $\lambda = 635$ and 405 nm . This result deserves some comments:

- 289 • The MAC value at $\lambda = 635 \text{ nm}$ differs for less than 3σ from the result reported in
290 (Massabò et al., 2016) and obtained in the same site and in a similar season (i.e.
291 November 2015 to January 2016; $MAC = 7.0 \pm 0.4 \text{ m}^2 \text{ g}^{-1}$). Since differences in the
292 type of wood burnt in the past and present campaign cannot be excluded, the two values
293 can be considered to be in fair agreement.
- 294 • No comparison with previous or other literature values is possible for the MAC value
295 at $\lambda = 405 \text{ nm}$, given the substantial differences in adopted definitions and
296 methodologies (Yang et al., 2009; Feng et al., 2013; Chen and Bond, 2010). However,
297 the increase by a factor 2.3 with respect to the MAC at $\lambda = 635 \text{ nm}$ follows the expected
298 behaviour.
- 299 • Under the assumption that the sole source of BrC is biomass burning, the MAC values
300 can be referred to the total concentration of organic carbon (i.e. including the part not
301 optically active) produced by biomass burning. Adopting with the present data set the
302 optical OC apportionment methodology reported in (Massabò et al., 2015), the BrC
303 values determined at $\lambda = 635 \text{ nm}$ turn out to be about 4% of the OC produced by wood



304 combustion, OC_{WB} , and consequently $MAC(OC_{WB}, @635nm) = 0.39 \pm 0.06 \text{ m}^2 \text{ g}^{-1}$.
305 When the analysis is performed at $\lambda = 405 \text{ nm}$, BrC results to be about 10% of OC_{WB}
306 and $MAC(OC_{WB}, @405nm) = 2.3 \pm 0.2 \text{ m}^2 \text{ g}^{-1}$. Previous literature works (Feng et al.,
307 2013; Laskin et al., 2015; and references therein) report MAC values of BrC and/or
308 related OC ranging in a quite large interval.

309 • The ratio between BrC and Levo concentration values results to be $BrC:Levo = 0.19 \pm$
310 0.02 and 0.42 ± 0.06 , respectively when considering the BrC concentration determined
311 by MWAA+Sunset at $\lambda = 635$ and 405 nm . In other words, the operative procedure,
312 introduced in (Massabò et al., 2016), results in different BrC concentration values
313 according to the considered/used wavelength. This fact can be interpreted in different
314 ways: while the analytical sensitivity is higher at $\lambda = 405 \text{ nm}$ and the corresponding
315 BrC values could be considered to be more firm, the category of compounds collected
316 under the label “Brow Carbon” could be itself “wavelength dependent”. The latter
317 would imply that the BrC concentration cannot be defined separately from the
318 wavelength and that its meaning is even more “operative” of the more widespread OC
319 and EC fractions. As a matter of fact, while the b_{abs}^{BrC} values discussed in section 3.3,
320 increase by a factor 5.8 moving from $\lambda = 635 \text{ nm}$ to $\lambda = 405 \text{ nm}$, the corresponding
321 variation of the $MAC(BrC)$ values is by a factor 2.3 only. This is because the BrC
322 concentration determined at $\lambda = 405 \text{ nm}$ doubles the value measured at $\lambda = 635 \text{ nm}$.
323 The purposes and the limits of the present study prevent any firm conclusion on the
324 alternative explanation: BrC definition is wavelength dependent or the analysis in red
325 light is not sensitive enough.

326 • When considering the $OC_{WB}:Levo$ concentration ratio, the MWAA analysis at $\lambda = 635$
327 and $\lambda = 405 \text{ nm}$ give well compatible results, with a mean value of $OC_{WB}:Levo = 4.5$
328 ± 0.5 .

329

330 4. Conclusions

331

332 We introduced a modified version of a commercial Sunset Lab. Inc. OC/EC Analyzer. We
333 upgraded the set-up of a standard unit making possible the alternative use of a red ($\lambda = 635$
334 nm) or blue ($\lambda = 405 \text{ nm}$) laser diode to monitor the light transmittance through the sample
335 during the thermal cycle. The analytical performance of the new set-up has been tested both
336 with artificial and real-world samples.



337 The new Sunset unit was used for the first time to analyze a set of samples collected mostly
338 wintertime in a mountain site of the Italian Apennines. Exploiting the synergic information
339 provided by the Multi Wavelength Absorbance Analyzer, MWAA (Massabò et al., 2015) and
340 adopting the procedure to retrieve the Brown Carbon concentration directly from the Sunset
341 thermograms (Massabò et al., 2016), we could measure the MAC(BrC) at the two wavelengths.
342 The result at $\lambda = 635$ nm ($\text{MAC} = 9.8 \pm 0.4 \text{ m}^2 \text{ g}^{-1}$) is in fair agreement with a previous study
343 performed in the same site in winter 2015-2016. At our knowledge, the result at $\lambda = 405$ nm,
344 $\text{MAC} = 23 \pm 1 \text{ m}^2 \text{ g}^{-1}$ is the sole direct observation at this wavelength.

345 In our analysis, the ratio between the BrC and the Levo concentration values depends on the
346 wavelength adopted during the thermo-optical analysis. This behaviour could be due to a better
347 accuracy of the results in blue-light, more sensitive at the BrC, or because the definition of BrC
348 itself has to be considered wavelength-dependent. The present results do not allow any
349 conclusive statement on this issue: actually, the label “Brown Carbon” as well as the widely
350 used “Organic and Elemental Carbon” comes from an operative definition not without
351 ambiguity.

352

353 **6. Acknowledgements**

354

355 This work has been partially financed by the National Institute of Nuclear Physics
356 (INFN) in the frame of the TRACCIA experiments.

357

358

359

360 **References**

361

362 Andreae, M. O. and Gelencsér, A.: Black Carbon or Brown Carbon? The nature of light-
363 absorbing carbonaceous aerosol, *Atmos. Chem. Phys.*, 6, 3131-3148, 2006.

364 Bernardoni, V., Pileci, R. E., Caponi, L., and Massabò, D.: The Multi-Wavelength Absorption
365 Analyzer (MWAA) model as a tool for source and component apportionment based on
366 aerosol absorption properties: application to samples collected in different environments,
367 *Atmosphere*, 8, 218, 2017.

368 Birch, M. E. and Cary, R. A.: Elemental carbon-based method for occupational monitoring of
369 particulate diesel exhaust: methodology and exposure issues, *Analyst*, 121, 1183-1190,
370 1996.



- 371 Bond, T. C. and Bergstrom, R. W.: Light absorption by carbonaceous particles: an investigative
372 review, *Aerosol Sci. Tech.*, 40, 27-67, 2006.
- 373 Bond, T. C. and Sun, H. L.: Can reducing black carbon emissions counteract global warming?,
374 *Environ. Sci. Technol.*, 39, 5921–5926, 2005.
- 375 Bond, T. C., Doherty, S. J., Fahey, D. W., Forster, P. M., Berntsen, T., De Angelo, B. J.,
376 Flanner, M. G., Ghan, S., Kärcher, B., Koch, D., Kinne, S., Kondo, Y., Quinn, P. K., Sarofim,
377 M. C., Schultz, M. G., Schulz, M., Venkataraman, C., Zhang, H., Zhang, S., Bellouin, N.,
378 Guttikunda, S. K., Hopke, P. K., Jacobson, M. Z., Kaiser, J. W., Klimont, Z., Lohmann, U.,
379 Schwarz, J. P., Shindell, D., Storelvmo, T., Warren, S. G., and Zender, C. S.: Bounding the
380 role of black carbon in the climate system: a scientific assessment, *J. Geophys. Res.-Atmos.*,
381 118, 5380-5552, 2013.
- 382 Bove, M. C., Brotto, P., Cassola, F., Cuccia, E., Massabò, D., Mazzino, A., Piazzalunga, A.,
383 and Prati, P.: An integrated PM_{2.5} source apportionment study: positive matrix factorisation
384 vs. the chemical transport model CAMx, *Atmos. Environ.*, 94, 274-286, 2014.
- 385 Cavalli, F., Putaud, J. P., Viana, M., Yttri, K. E., and Gemberg, J.: Toward a standardized
386 thermal-optical protocol for measuring atmospheric Organic and Elemental Carbon: the
387 EUSAAR protocol, *Atmos. Meas. Tech.*, 3, 79-89, 2010.
- 388 Chen, Y. and Bond, T. C.: Light absorption by organic carbon from wood combustion, *Atmos.*
389 *Chem. Phys.*, 10, 1773–1787, 2010.
- 390 Chen, L. W. A., Chow, J. C., Wang, X. L., Robles, J. A., Sumlin, B. J., Lowenthal, D. H.,
391 Zimmermann, R., and Watson, J. G.: Multi-wavelength optical measurement to enhance
392 thermal/optical analysis for carbonaceous aerosol, *Atmos. Meas. Tech.*, 8, 451-461, 2015.
- 393 Chow, J. C., Watson, J. G., Chen, L. W. A., Arnott, W. P., Moosmüller, H., and Fung, K. K.:
394 Equivalence of elemental carbon by thermal/optical reflectance and transmittance with
395 different temperature protocols, *Environ. Sci. Technol.*, 38, 4414-4422, 2004.
- 396 Chow, J. C., Watson, J. G., Mauderly, J. L., Costa, D. L., Wyzga, R. E., Vedal, S., Hidy, G.
397 M., Altshuler, S. L., Marrack, D., Heuss, J. M., Wolff, G. T., Pope, C. A. III, and Dockery,
398 D. W.: Health effects of fine particulate air pollution: lines that connect, *J. Air Waste Manag.*
399 *Assoc.*, 56, 1368–1380, 2006.
- 400 Chow, J. C., Watson, J. G., Chen, L. W. A., Chang, M. C. O., Robinson, N. F., Trimble, D. L.,
401 and Kohl, S. D.: The IMPROVE_A temperature protocol for thermal/optical carbon analysis:
402 maintaining consistency with a long-term database, *J. Air Waste Manag. Assoc.*, 57, 1014-
403 1023, 2007.



- 404 Chow, J. C., Watson, J. G., Lowenthal, D. H., Chen, L. W. A., and Motallebi, N.: Black and
405 organic carbon emission inventories: review and application to California, *J. Air Waste*
406 *Manag. Assoc.*, 60, 497–507, 2010.
- 407 Chow, J. C., Wang, X., Sumlin, B. J., Gronstal, S. B., Chen, L. W. A., Trimble, D. L., Kohl, S.
408 D., Mayorga, S. R., Riggio, G., Hurbain, P. R., Johnson, M., Zimmermann, R., and Watson,
409 J. G.: Optical calibration and equivalence of a multiwavelength thermal/optical carbon
410 analyzer, *Aerosol Air Qual. Res.*, 15, 1145–1159, 2015.
- 411 Chow, J. C., Watson, J. G., Green, M. C., Wang, X., Chen, L. W. A., Trimble, D. L., Cropper,
412 P. M., Kohl S. D., and Gronstal, S. B.: Separation of brown carbon from black carbon for
413 IMPROVE and Chemical Speciation Network PM_{2.5} samples, *J. Air Waste Manag. Assoc.*,
414 68:5, 494–510, 2018.
- 415 Corbin J. C., Pieber S. M., Czech H., Zanatta M., Jakobi G., Massabò D., Orasche J., El
416 Haddad I., Mensah A. A., Stengel B., Drinovec L., Mocnik G., Zimmermann R., Prévôt
417 A. S. H., and M. Gysel: Brown and Black Carbon emitted by a marine engine operated on
418 heavy fuel oil and distillate fuels: optical properties, size distributions, and emission factors,
419 *J. Geophys. Res-Atmos*, 123, 6175–6195, 2018.
- 420 Daellenbach, K.R., Bozzetti, C., Křepelová, A., Canonaco, F., Wolf, R., Zotter, P., Fermo, P.,
421 Crippa, M., Slowik, J.G., Sosedova, Y., Zhang, Y., Huang, R. J., Poulain, L., Szidat, S.,
422 Baltensperger, U., El Haddad, I., and Prévôt, A. S. H.: Characterization and source
423 apportionment of organic aerosol using offline aerosol mass spectrometry, *Atmos. Meas.*
424 *Tech.*, 9 (1), 23–39, 2016.
- 425 Favez, O., El Haddad, I., Piot, C., Boreave, A., Abidi, E., Marchand, N., Jaffrezo, J. L.,
426 Besombes, J. L., Personnaz, M. B., Sciare, J., Wortham, H., Geroge, C., and D’Anna, B.:
427 Inter-comparison of source apportionment models for the estimation of wood burning
428 aerosols during wintertime in an Alpine city (Grenoble, France), *Atmos. Chem. Phys.*, 10,
429 5295–5314, 2010.
- 430 Feng, Y., Ramanathan, V., and Kotamarthi, V. R.: Brown carbon: a significant atmospheric
431 absorber of solar radiation?, *Atmos. Chem. Phys.*, 13, 8607–8621, 2013.
- 432 Ferrero, L., Močnik, G., Cogliati, S., Gregorič, A., Colombo, R., and Bolzacchini, E.: Heating
433 rate of light absorbing aerosols: time-resolved measurements, the role of clouds, and source
434 identification, *Environ. Sci. Tech.*, 52 (6), 3546–3555, 2018.
- 435 Filep, Á., Ajtai, T., Utry, N., Pintér, M. D., Nyilas, T., Takács, S., Máté, Z., Gelencsér, A.,
436 Hoffer, A., Schnaiter, M., Bozóki, Z., and Szabó, G.: Absorption spectrum of ambient



- 437 aerosol and its correlation with size distribution in specific atmospheric conditions after a
438 red mud accident, *Aerosol Air Qual. Res.*, 13, 49-59, 2013.
- 439 Harrison, R. M., Beddows, D. C. S., Jones A. M., Calvo A., Alves C., and Pio C.: An evaluation
440 of some issues regarding the use of aethalometers to measure woodsmoke concentrations,
441 *Atmos. Environ.*, 80, 540-548, 2013.
- 442 Highwood, E. J. and Kinnersley, R. P.: When smoke gets in our eyes: the multiple impacts of
443 atmospheric black carbon on climate, air quality and health, *Environ. Int.*, 32, 560–566,
444 2006.
- 445 Hitzenberger, R., Petzold, A., Bauer, H., Ctyroky, P., Pouresmaeil, P., Laskus, L., and
446 Puxbaum, H.: Intercomparison of thermal and optical measurement methods for elemental
447 carbon and black carbon at an urban location, *Environ. Sci. Technol.*, 40 (20), 6377-6383,
448 2006.
- 449 Karanasiou, A., Minguillon, M. C., Viana, M., Alaustey, A., Puaud, J. P., Maenhaut, W.,
450 Panteliadis, P., Močnik, G., Favez, O., and Kuhlbusch, T. A.: Thermal-optical analysis for
451 the measurement of elemental carbon (EC) and organic carbon (OC) in ambient air, a
452 literature review, *Atmos. Meas. Tech. Discuss.*, 8, 9649-9712, 2015.
- 453 Kirchstetter, T. W., Novakok, T., and Hobbs, P. V.: Evidence that the spectral dependence of
454 light absorption by aerosols is affected by organic carbon, *J. Geophys. Res.*, 109, D21208,
455 2004.
- 456 Lack, D. A., Langridge, J. M., Bahreini, R., Cappa, C. D., Middlebrook, A. M., and Schwarz,
457 J. P.: Brown carbon and internal mixing in biomass burning particles, *Proc. Natl. Acad. Sci.*,
458 109, 14802-14807, 2012.
- 459 Lack, D. A. and Langridge, J. M.: On the attribution of black and brown carbon light absorption
460 using the Ångström exponent, *Atmos. Chem. Phys.*, 13, 10535-10543, 2013.
- 461 Laskin, A., Laskin, J., and Nizkorodov S. A.: Chemistry of atmospheric brown carbon, *Chem.*
462 *Rev.*, 115 (10), 4335–4382, 2015.
- 463 Lewis, K., Arnott, W. P., Moosmüller, H., and Wold, C. E.: Strong spectral variation of
464 biomass smoke light absorption and single scattering albedo observed with a novel dual-
465 wavelength photoacoustic instrument, *J. Geophys. Res.*, 113, D16203, 2008.
- 466 Massabò, D., Bernardoni, V., Bove, M. C., Brunengo, A., Cuccia, E., Piazzalunga, A., Prati,
467 P., Valli, G., and Vecchi, R.: A multi-wavelength optical set-up for the characterization of
468 carbonaceous particulate matter, *J. Aerosol Sci.*, 60, 34-46, 2013.
- 469 Massabò, D., Caponi, L., Bernardoni, V., Bove, M. C., Brotto, P., Calzolari, G., Cassola, F.,
470 Chiari, M., Fedi, M. E., Fermo, P., Giannoni, M., Lucarelli, F., Nava, S., Piazzalunga, A.,



- 471 Valli, G., Vecchi, R., and Prati, P.: Multi-wavelength optical determination of black and
472 brown carbon in atmospheric aerosols, *Atmos. Environ.*, 108, 1-12, 2015.
- 473 Massabò, D., Caponi, L., Bove, M. C., and Prati, P.: Brown carbon and thermal-optical
474 analysis: a correction based on optical multi-wavelength apportionment of atmospheric
475 aerosols, *Atmos. Environ.*, 125, 119-125, 2016.
- 476 Mauderly, J. L. and Chow, J. C.: Health effects of organic aerosols, *Inhal. Toxicol.*, 20, 257–
477 288, 2008.
- 478 Moosmüller, H., Chakrabarty, R. K., and Arnott, W. P.: Aerosol light absorption and its
479 measurement: a review, *J. Quant. Spectrosc. Ra.*, 110, 844-878, 2009.
- 480 Moosmüller, H., Chakrabarty, R. K., Ehlers, K. M., and Arnott, W. P.: Absorption Ångström
481 coefficient, brown carbon, and aerosols: basic concepts, bulk matter, and spherical particles,
482 *Atmos. Chem. Phys.*, 11, 1217-1225, 2011.
- 483 Olson, M. R., Garcia, M. V., Robinson, M. A., Van Rooy, P., Dietenberger, M. A., Bergin, M.,
484 and Schauer, J. J.: Investigation of black and brown carbon multiple-wavelength-dependent
485 light absorption from biomass and fossil fuel combustion source emissions, *J. Geophys. Res.*
486 *Atmos.*, 120, 2015.
- 487 Panteliadis, P., Hafkenschied, T., Cary, B., Diapouli, E., Fischer, A., Favez, O., Quincey, P.,
488 Viana, M., Hitzenberger, R., Vecchi, R., Saraga, D., Sciare, J., Jaffrezo, J. L., John, A.,
489 Schwarz, J., Giannoni, M., Novak, J., Karanasiou, A., Fermo, P., and Maenhaut, W.: ECOC
490 comparison exercise with identical thermal protocols after temperature offset correction –
491 instrument diagnostics by in-depth evaluation of operational parameters, *Atmos. Meas.*
492 *Tech.*, 8, 779–792, 2015.
- 493 Piazzalunga, A., Fermo, P., Bernardoni, V., Vecchi, R., Valli, G., and De Gregorio M. A.: A
494 simplified method for levoglucosan quantification in wintertime atmospheric particulate
495 matter by high performance anion-exchange chromatography coupled with pulsed
496 amperometric detection, *Int. J. Environ. An. Ch.*, 90, 934-947, 2010.
- 497 Piazzalunga, P., Bernardoni, V., Fermo, P., Valli, G., and Vecchi, R.: On the effect of water-
498 soluble compounds removal on EC quantification by TOT analysis in urban aerosol samples,
499 *Atmos. Chem. Phys.*, 11, 10193-10203, 2011.
- 500 Pope, C. A. III and Dockery, D. W.: Health effects of fine particulate air pollution: lines that
501 connect, *J. Air Waste Manag. Assoc.*, 56, 709–742, 2006.
- 502 Pöschl, U.: Aerosol particle analysis: challenges and progress, *Anal. Bioanal. Chem.*, 375,
503 3032, 2003.



- 504 Sandradewi, J., Prevot, A. H., Szidat, S., Perron, N., Rami Alfarra, M., Lanz, V., Weingartner,
505 E., and Baltensperger, U.: Using aerosol light absorption measurements for the quantitative
506 determination of wood burning and traffic emission contributions to particulate matter,
507 Environ. Sci. Technol., 3316-3323, 2008.
- 508 Subramanian, R., Khlystov, A. Y., and Robinson, A. L.: Effect of peak inert-mode temperature
509 on elemental carbon measured using thermal-optical analysis, Aerosol Sci. Tech., 40, 763–
510 780, 2006.
- 511 Utry, N., Ajtai, T., Filep, Á., Dániel P. M., Hoffer, A., Bozoki, Z., and Szabó, G.: Mass specific
512 optical absorption coefficient of HULIS aerosol measured by a four-wavelength
513 photoacoustic spectrometer at NIR, VIS and UV wavelengths, Atmos. Environ., 69, 321-
514 324, 2013.
- 515 Utry, N., Ajtai, T., Filep, Á., Pintér, M., Török, Zs., Bozóki, Z., and Szabó, G.: Correlations
516 between absorption Angström exponent (AAE) of wintertime ambient urban aerosol and its
517 physical and chemical properties, Atmos. Environ., 91, 52-59, 2014.
- 518 Vassura, I., Venturini, E., Marchetti, S., Piazzalunga, A., Bernardi, E., Fermo, P., and Passarini,
519 F.: Markers and influence of open biomass burning on atmospheric particulate size and
520 composition during a major bonfire event, Atmos. Environ., 82, pp. 218-225, 2014.
- 521 Watson, J. G., Chow, J. C., and Chen, L. W. A.: Summary of organic and elemental
522 carbon/black carbon analysis methods and intercomparisons, Aerosol Air Qual. Res., 5, 65-
523 102, 2005.
- 524 Yang, H. and Yu, J. Z.: Uncertainties in charring correction in the analysis of elemental and
525 organic carbon in atmospheric particles by thermal/optical methods, Environ. Sci. Technol.,
526 36, 5199-5204, 2002.
- 527 Yang, M., Howell, S. G., Zhuang, J., and Huebert, B. J.: Attribution of aerosol light absorption
528 to black carbon, brown carbon, and dust in China - interpretations of atmospheric
529 measurements during EAST-AIRE, Atmos. Chem. Phys., 9, 2035-2050, 2009.
- 530 Zheng, G., He, K., Duan, F., Cheng, Y., and Ma, Y.: Measurement of humic-like substances in
531 aerosols: A review, Environ. Pollut., 181, 301-314, 2013.
- 532 Zhi, G., Chen, Y., Sheng, G., and Fu, J.: Effects of temperature parameters on thermal-optical
533 analysis of organic and elemental carbon in aerosol, Environ. Monit. Assess., 154, 253–
534 261, 2008.



535 **FIGURE CAPTIONS**

536

537 **Figure 1:** The new $\lambda = 405$ nm laser diode mounted by a steel adapter on the SUNSET furnace
538 (top) and the comparison with the standard $\lambda = 635$ nm laser diode implemented by the
539 manufacturer (bottom).

540

541 **Figure 2:** Quantification of TC (primary axis) and EC (secondary axis) at $\lambda = 635$ nm (red) and
542 $\lambda = 405$ nm (blue) for the set of synthetic Aquadag samples. Top: NIOSH5040 protocol,
543 bottom: EUSAAR_2 protocol.

544

545 **Figure 3:** Quantification of TC (primary axis) and EC (secondary axis) at $\lambda = 635$ nm (red) and
546 $\lambda = 405$ nm (blue) for the set of synthetic Aquadag + Ammonium Sulphate samples by the
547 EUSAAR_2 protocol.

548 **Figure 4:** EC concentration measured in two sub-sets of PM10 samples collected in
549 consecutive days in the urban area of Genoa in late spring 2016. Values determined with the
550 Sunset analyzer equipped with blue and red laser diodes, are compared.

551

552 **Figure 5:** Primary axis: Optical apportionment of the aerosol absorption coefficient (b_{abs}) @ λ
553 = 635 nm (top) and $\lambda = 405$ nm (bottom). Secondary axis: experimental AAE values obtained
554 by fitting the measured b_{abs} values with a power-law relationship $b_{\text{abs}}(\lambda) \sim \lambda^{-\text{AAE}}$. WW and FF
555 stand for Fossil Fuel and Wood Burning, respectively.

556

557 **Figure 6:** Aerosol absorption coefficient apportioned to Brown Carbon ($b_{\text{abs}}^{\text{BrC}}$) @635 nm (top)
558 and @405 nm (bottom) vs. levoglucosan concentration.

559

560 **Figure 7:** Comparison between the aerosol absorption coefficient apportioned to Brown
561 Carbon vs. the resulting operative BrC concentration values @635 nm (top) and @405 nm
562 (bottom).

563

564

565

566



567

568 Figure 1

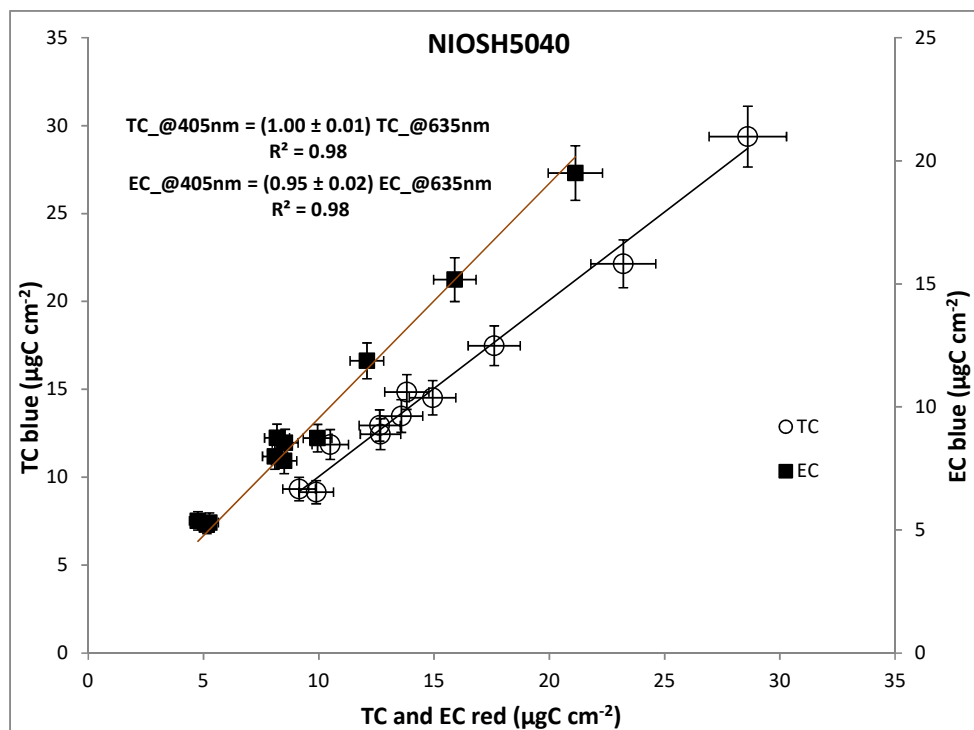
569

570

571



572



573
574

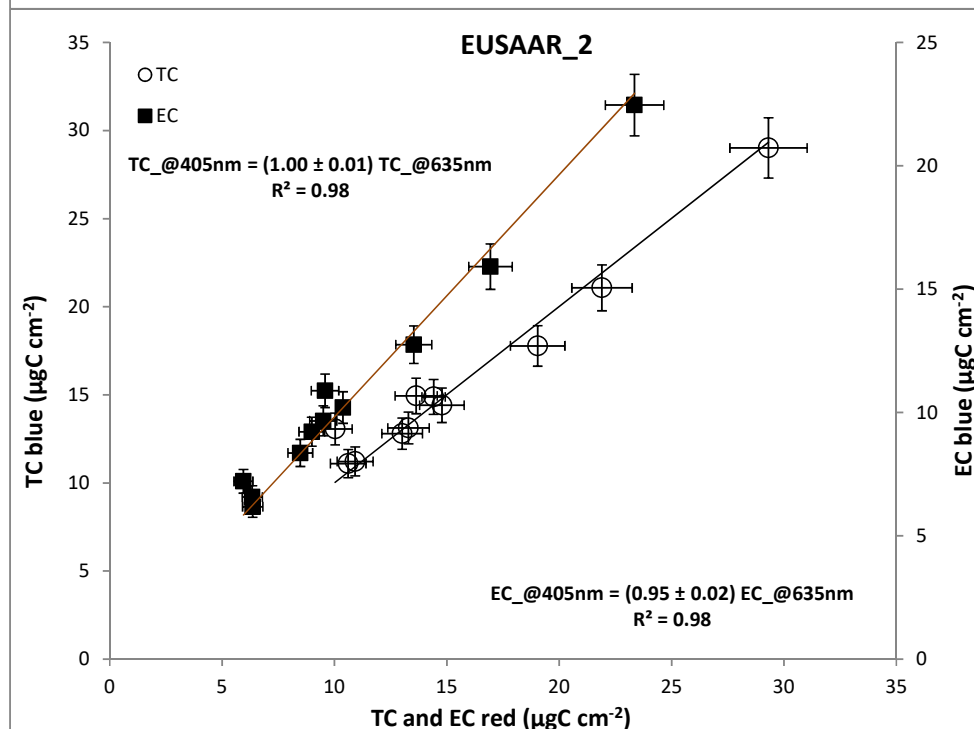
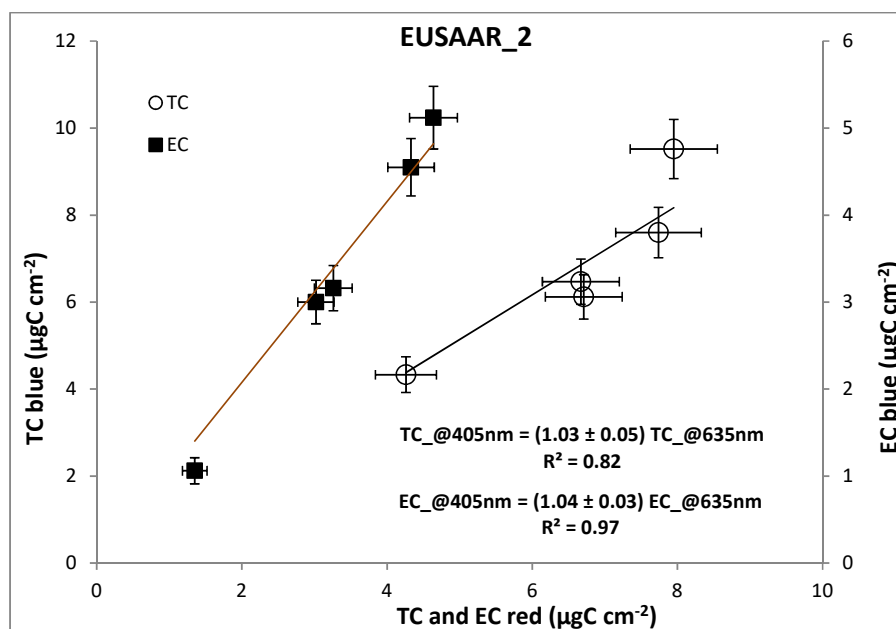


Figure 2

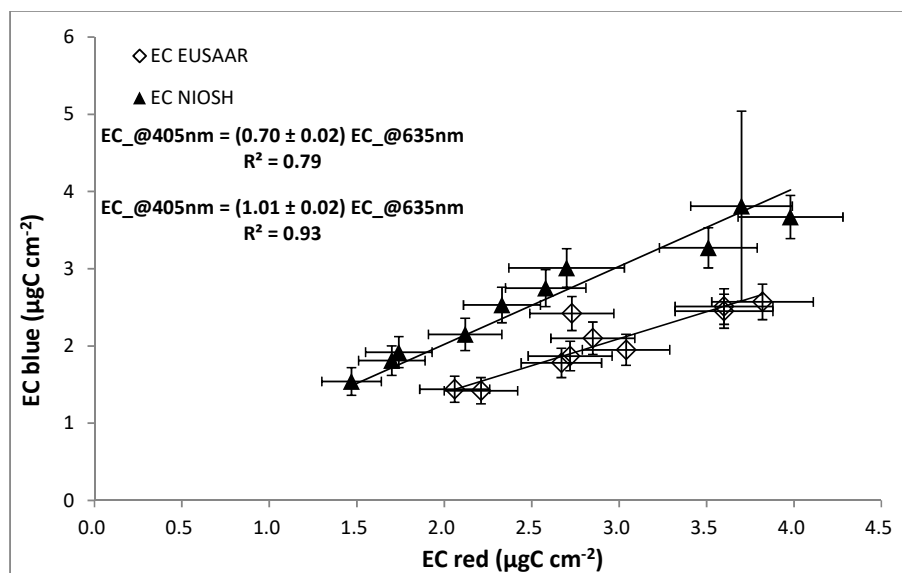


575



576
 577

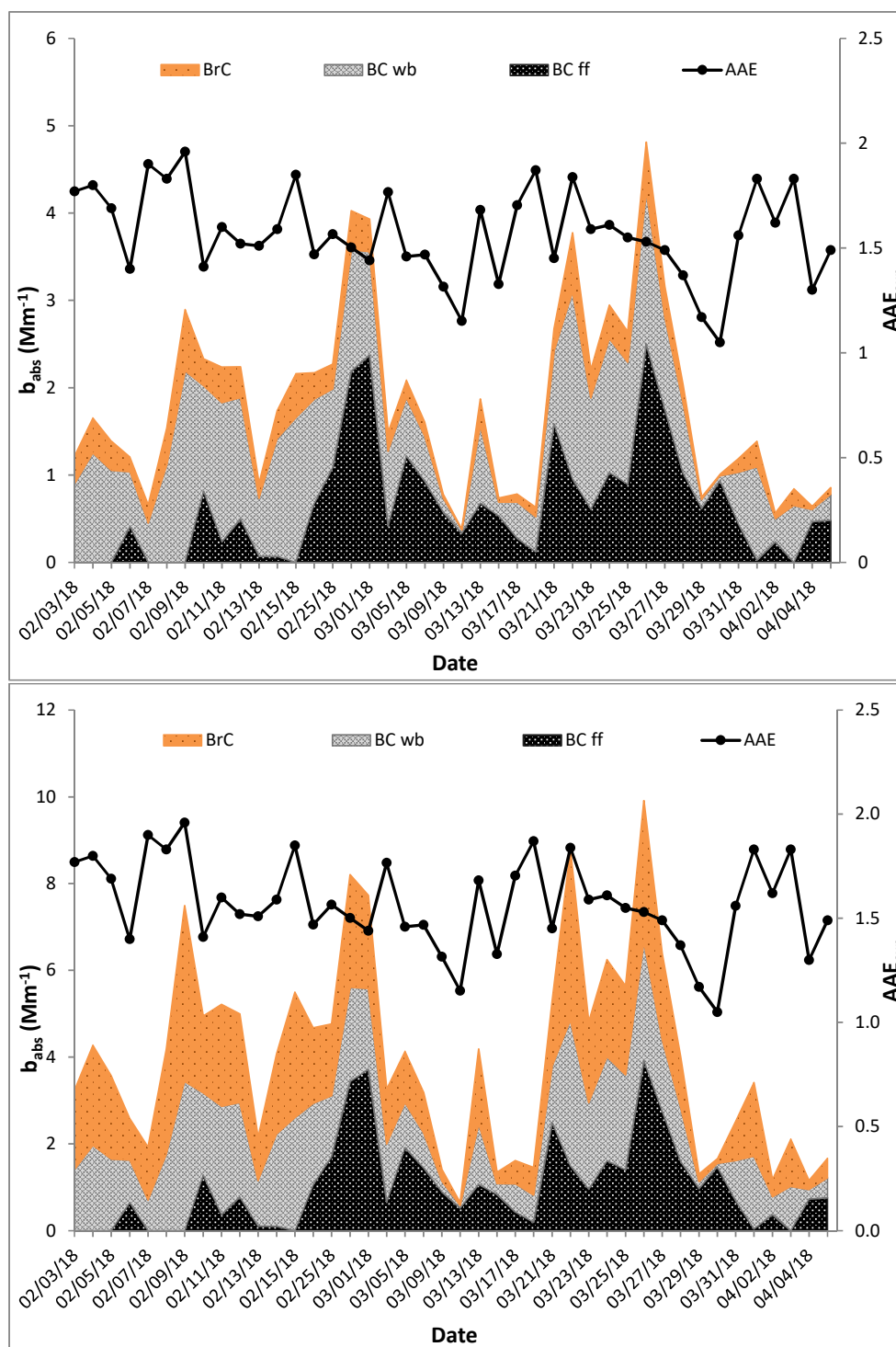
Figure 3



578
 579

Figure 4

580



581

582
 583

Figure 5

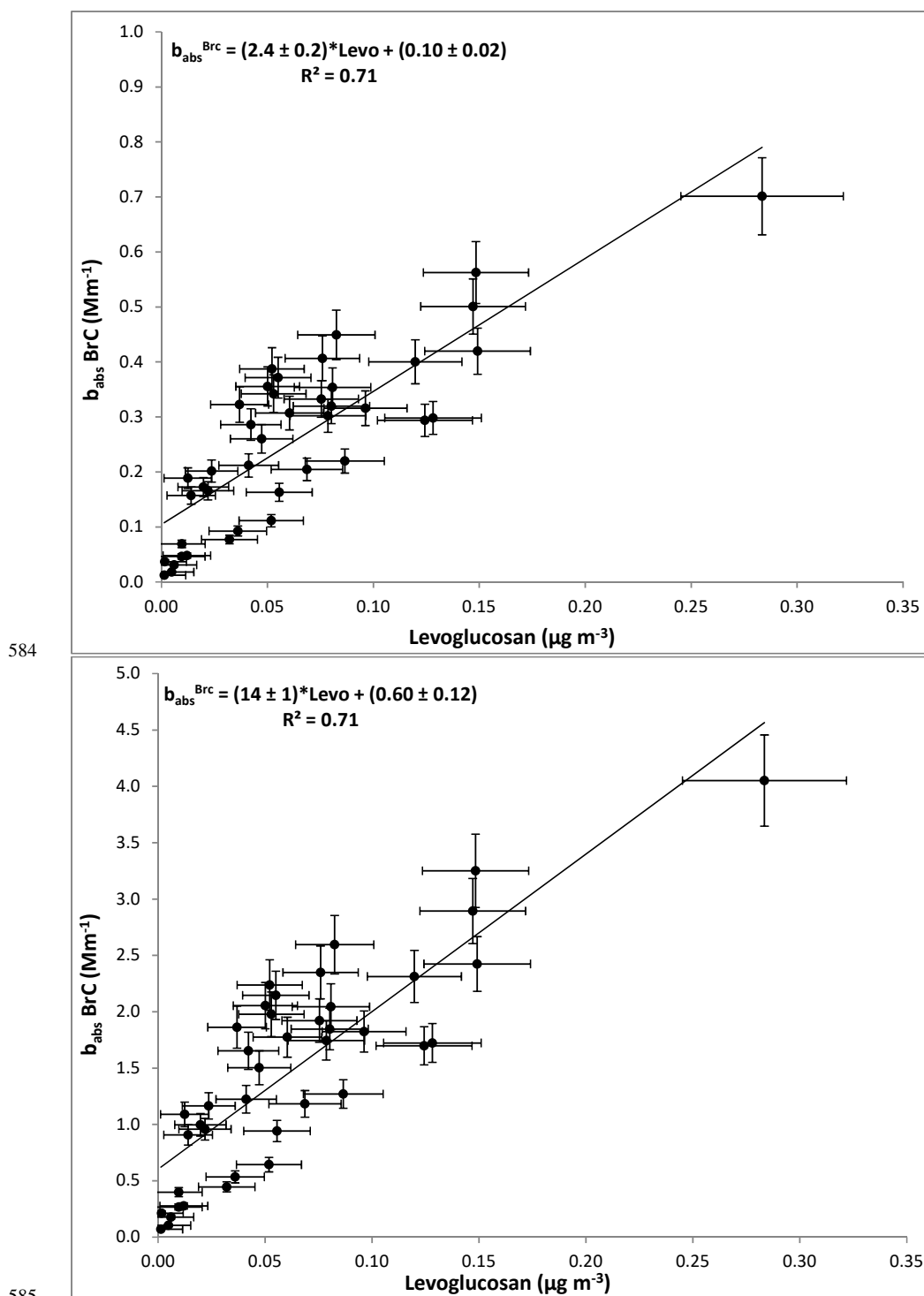


Figure 6

